Mechanisms of CO_2/H^+ chemoreception by respiratory rhythm generator neurons in the medulla from newborn rats *in vitro*

Akira Kawai[1,2], Hiroshi Onimaru[1] and Ikuo Homma[1]

[1]*Department of Physiology, Showa University School of Medicine, Tokyo 142-8555, Japan*
[2]*Department of Respiratory Medicine, Kawai Medical Clinic, Tokyo 167-0043, Japan*

We investigated mechanisms of CO_2/H^+ chemoreception in the respiratory centre of the medulla by measuring membrane potentials of pre-inspiratory neurons, which are putative respiratory rhythm generators, in the brainstem–spinal cord preparation of the neonatal rat. Neuronal response was tested by changing superfusate CO_2 concentration from 2% to 8% at constant HCO_3^- concentration (26 mM) or by changing pH from 7.8 to 7.2 by reducing HCO_3^- concentration at constant CO_2 (5%). Both respiratory and metabolic acidosis lead to depolarization of neurons with increased excitatory synaptic input and increased burst rate. Respiratory acidosis potentiated the amplitude of the neuronal drive potential. In the presence of tetrodotoxin (TTX), membrane depolarization persisted during respiratory and metabolic acidosis. However, the depolarization was smaller than that before application of TTX, which suggests that some neurons are intrinsically, and others synaptically, chemosensitive to CO_2/H^+. Application of Ba^{2+} blocked membrane depolarization by respiratory acidosis, whereas significant depolarization in response to metabolic acidosis still remained after application of Cd^{2+} and Ba^{2+}. We concluded that the intrinsic responses to CO_2/H^+ changes were mediated by potassium channels during respiratory acidosis, and that some other mechanisms operate during metabolic acidosis. In low-Ca^{2+}, high-Mg^{2+} solution, an increased CO_2 concentration induced a membrane depolarization with a simultaneous increase of the burst rate. Pre-inspiratory neurons could adapt their baseline membrane potential to external CO_2/H^+ changes by integration of these mechanisms to modulate their burst rates. Thus, pre-inspiratory neurons might play an important role in modulation of respiratory rhythm by central chemoreception in the brainstem–spinal cord preparation.

(Resubmitted 27 November 2005; accepted after revision 6 February 2006; first published online 9 February 2006)
Corresponding author H. Onimaru: Department of Physiology, Showa University, School of Medicine, Tokyo 142-8555, Japan. Email: oni@med.showa-u.ac.jp

Neuronal mechanisms of central chemoreception of respiration are not fully understood. Chemosensitive regions have been found in the ventral medullary surface (Mitchell *et al.* 1963; Schlaefke *et al.* 1970; Loeschcke *et al.* 1970). Because no intrinsically chemosensitive neuron has been identified there, Loeschcke (1982) suggested that the synaptic mechanism located in the chemosensitive areas of the ventral surface of the medulla is responsible for the chemosensitivity of respiration. Chemosensitive sites have also been found in the nucleus tractus solitarii (NTS), the medullary raphe, the retrotrapezoid nucleus (RTN), the rostral aspect of the ventral respiratory group, the pre-Bötzinger complex, the fastigial nucleus of the cerebellum and the region of the locus coeruleus (Dean *et al.* 1989; Coates *et al.* 1993; Kawai *et al.* 1996; Oyamada *et al.* 1998; Nattie, 1999, 2000, 2001; Nattie & Li, 2002). Intrinsic chemosensitive neurons have been found in the NTS (Dean *et al.* 1989, 1990) as well as in the ventral respiratory area and ventral surface (Onimaru *et al.* 1989; Kawai *et al.* 1996; Okada *et al.* 2002). Recently, Mulkey *et al.* (2004) found intrinsic CO_2-sensitive neurons in the RTN that were located close to the ventral surface of the rostral medulla. Serotonergic neurons in the medulla have also been shown to be chemosensitive to CO_2/H^+ (Richerson, 2004). These chemosensitive neurons might be the primary chemoreceptors of respiration. Although such neurons are intrinsically chemosensitive to CO_2/H^+, the neuronal mechanisms mediating an increase in respiratory rhythm in response to hypercapnia are unknown. In a recent review, Feldman *et al.* (2003) emphasized that

 DOI: 10.1113/jphysiol.2005.102533

many cell types and molecular mechanisms are involved in respiratory chemoreception.

The *in vitro* brainstem–spinal cord preparation from newborn rat is known to respond to hypercapnia mainly by an increase in respiratory frequency (Issa & Remmers, 1992; Okada *et al.* 1993*b*; Kawai *et al.* 1996); however, it has also been suggested that the amplitude of phrenic nerve activity could increase independently in response to hypercapnia (Harada *et al.* 1985). In the awake adult rat preparation, hypercapnia increases both respiratory frequency and tidal volume (Li & Nattie, 2002). The *in vivo* vagotomised cat preparation, tidal volume is known to increase only in response to hypercapnia. Focal stimulation of the RTN in the awake rat increases tidal volume alone (Li *et al.* 1999), whereas focal stimulation of the NTS increases both respiratory frequency and tidal volume (Nattie & Li, 2002). The NTS and the carotid body or another central chemoreceptor site of the brainstem may contribute to the response of respiratory frequency (Li & Nattie, 2002). The *in vitro* brainstem–spinal cord preparation from newborn rat does not have the carotid body and contains the NTS as well as many chemoreceptor sites of the medulla. Because the *in vitro* preparation spontaneously generates a respiratory rhythm for more than 8 h and extracellular conditions can easily be modified, the preparation is useful for pursuit of the neuronal mechanisms of CO_2/H^+ chemoreception and respiratory rhythm modulation (Suzue, 1984; Ballanyi *et al.* 1999).

Because respiratory rhythm of the neonatal rat is thought to be generated in the rostral ventrolateral medulla (RVL) (Onimaru *et al.* 1987; Errchidi *et al.* 1991; Ballanyi *et al.* 1999) or the pre-Bötzinger complex (Smith *et al.* 1991), or in both (Mellen *et al.* 2003; Feldman *et al.* 2003), chemosensitive neurons in these regions and chemosensitive neurons having connection with these regions are expected to be important modulators of the basic respiratory rhythm. Pre-inspiratory (Pre-I) neurons located in the RVL, including the recently identified para-facial respiratory group (pFRG; Onimaru & Homma, 2003), constitute a crucial part of the respiratory neuronal network and contribute to respiratory rhythmogenesis in the neonatal rat brainstem. We have proposed that Pre-I neurons are the primary respiratory rhythm generators and that they determine basic respiratory rhythm by triggering inspiratory activity in the brainstem–spinal cord preparation (reviewed by Ballanyi *et al.* (1999)). Therefore, clarification of the mechanisms of CO_2/H^+ chemoreception by Pre-I neurons is necessary for understanding modulation of respiratory rhythm by changes in CO_2/H^+ in this preparation. The neuronal mechanisms of chemoreception by Pre-I neurons have not been examined systematically and the channels involved in chemoreception have never been elucidated. Thus, we tested the response of Pre-I neurons to both respiratory and metabolic acidosis and determined whether the responses were mediated by intrinsic or synaptic mechanisms, or by both. Furthermore, we examined the channel mechanisms that are responsible for chemoreception. Some of our results have appeared in abstract form (Kawai *et al.* 1997).

Methods

Preparation and solutions

We used 60 neonatal Wistar rats. Experimental protocols were approved by the Animal Research Committee of Showa University, which operates in accordance with Japanese Government Law no. 105. Each neonatal albino rat (0–4 days old) was anaesthetized with ether. The brainstem was decerebrated rostrally between the VIth cranial nerve roots and the lower border of the trapezoid body. The brainstem and spinal cord were transferred to the recording chamber (volume, 2 ml) ventral side up and superfused with artificial cerebrospinal fluid (CSF) at a rate of 7 ml min^{-1}. This control solution contained (mM): NaCl 124, KCl 5.0, KH_2PO_4 1.2, $CaCl_2$ 2.4, $MgSO_4$ 1.3, $NaHCO_3$ 26 and glucose 30, and was equilibrated with 90% O_2–5% CO_2–5% N_2. pH was 7.4 at the experimental temperature of 25–26°C.

The control CSF solution was replaced by several test CSF solutions that differed in either the CO_2 or HCO_3^- concentration. The following solutions were used: hypercapnic acidic CSF equilibrated with 8% CO_2 (pH 7.2) as a model for respiratory acidosis; hypocapnic alkaline CSF equilibrated with 2% CO_2 (pH 7.8) as a model for respiratory alkalosis; normocapnic acidic CSF containing 13 mM HCO_3^- (pH 7.2) as a model for metabolic acidosis; and normocapnic alkaline CSF containing 52 mM HCO_3^- (pH 7.8) as a model for metabolic alkalosis. Additional solutions were equilibrated with the same gas mixture as above and contained tetrodotoxin (TTX; 0.5–1.0 μM, Sigma), $CdCl_2$ (0.2 mM), $BaCl_2$ (1–2 mM), or low Ca^{2+} (0.2 mM) and elevated Mg^{2+} (5 mM) levels (referred to as low-Ca solution).

Measurement techniques

pH of the superfusate was measured continuously in the recording chamber or on the ventral surface of the medulla with a microelectrode (MI-410, Microelectrodes, Inc., Bedford, NH, USA) calibrated with standard phosphate buffers. Inspiratory electrical activities of the phrenic efferent fibres were recorded from C4 ventral roots with glass suction electrodes. The respiratory frequency was defined as the frequency of the C4 bursts. The method of intracellular recording of Pre-I neurons has been previously described (Onimaru & Homma, 1992). Briefly, electrodes were pulled in one stage from thin-walled borosilicate glass (GC100TF-10, with filament, Clark

Electromed, Reading, UK) on a vertical puller (PE-2, Narishige, Tokyo, Japan) at a heat setting of 12 A. Electrodes had tip inner diameters between 1.2 and 2.0 μm and resistances of 4–8 MΩ. Electrodes were filled with the following solution (mM): potassium gluconate 130, EGTA 10, Hepes 10, $CaCl_2$ 1, $MgCl_2$ 1, Na_2-ATP 1 and 0.5%Lucifer Yellow. pH was adjusted to 7.2–7.3 with KOH.

Electrodes were inserted into the rostral ventrolateral medulla around the caudal end of the facial nucleus at the level of the roots of nerves IX and X (Onimaru *et al.* 1987; Arata *et al.* 1990), corresponding to the caudal part of the pFRG (Onimaru & Homma, 2003), through a small region where the pia was removed. Pre-I neurons were sought by advancing the electrode while monitoring amplified extracellular signals with a sound monitor. A single-electrode voltage-clamp amplifier (CEZ-3100, Nihon Koden, Tokyo, Japan) was used for recording of both extracellular signals and intracellular membrane potentials in the whole-cell configuration after compensation for series resistance (20–50 MΩ) and capacitance. Membrane potentials were not corrected for liquid-junction potentials (Onimaru & Homma, 1992; Onimaru *et al.* 2003). We analysed changes in the magnitude of the drive potential which was defined as the voltage difference between the resting membrane potential in the interburst phase and the peak of the plateau depolarization during a pre- or post-inspiratory burst phase of Pre-I neurons (Onimaru *et al.* 2003). We also analysed intraburst spike frequency. Mean values were calculated from five consecutive respiratory cycles. To analyse post synaptic currents in some experiments, membrane currents were recorded in the discontinuous voltage-clamp mode (switching frequency, 10 kHz) at a membrane potential of −55 mV.

Experimental protocol

After the preparation had stabilized in the recording chamber with control CSF, C4 output and intracellular membrane potential were measured for 10 min. Control CSF was then replaced by a test solution. Response to the test solution was recorded for 5–10 min. In each preparation, test solutions were applied in one or more of the following five sequences. Sequence 1 (to test the response to respiratory acidosis and alkalosis): control CSF → hypocapnic alkaline CSF → hypercapnic acidic CSF → hypocapnic alkaline CSF → control CSF. Sequence 2 (to test the response to metabolic acidosis and alkalosis): control CSF → normocapnic alkaline CSF → normocapnic acidic CSF → normocapnic alkaline CSF → control CSF. Sequence 3 (to test the response to changes in CO_2 level at the same pH): control CSF → hypocapnic alkaline CSF → normocapnic alkaline CSF → normocapnic acidic CSF → hypercapnic acidic CSF. Sequence 4 (to investigate the channel mechanisms that mediated the responses to respiratory or metabolic acidosis): control CSF + TTX → control CSF + TTX + Cd^{2+} → control CSF + TTX + Cd^{2+} + Ba^{2+}. Sequence 5 (to study intrinsic burst-generating properties of Pre-I neurons in response to respiratory or metabolic acidosis): control CSF → low-Ca CSF → hypocapnic, alkaline, low-Ca CSF → hypercapnic, acidic, low-Ca CSF → hypocapnic, alkaline, low-Ca CSF → control CSF → low-Ca CSF → normocapnic, low-Ca, alkaline CSF → normocapnic, acidic, low-Ca CSF → normocapnic, alkaline, low-Ca CSF → control CSF.

The order of Sequences 1–3 was randomised to avoid time-dependent effects, whereas Sequences 4 and 5 were tested at the end of the experiment. When the preparation did not recover to the control baseline, the experiment was discontinued and the data were excluded from analysis. In all, 60 preparations were successfully tested with some sequences. Values are presented as the mean ± standard deviation (S.D.). The mean values of multiple observations were compared by two-way analysis of variance with repeated measures. The significance of differences ($P < 0.05$) between control and test groups was estimated with paired or unpaired student's *t* test.

Histology

Lucifer Yellow was injected by current pulses during and after the recording period. After the experiment, the preparation was fixed for more than 48 h at 4°C in Lillie's solution (10% formalin in phosphate buffer, pH 7.2). It was rinsed with 15% sucrose–0.1 M phosphate buffer (pH 7.2) and then immersed overnight in sucrose solution. Transverse 70-μm frozen sections were then cut on a cryostat. The stained neurons were photographed through a fluorescence microscope, and selected neurons were traced with a camera lucida.

Results

General features of the C4 response to respiratory and metabolic acidosis

Both respiratory and metabolic acidosis increased C4 burst frequency of respiratory activity in this preparation (Table 1). The amplitude of the C4 burst was not consistently altered by either respiratory or metabolic acidosis (Fig. 1). At constant HCO_3^- concentration (26 mM), the respiratory frequency increased significantly at 8% CO_2 (pH 7.2, respiratory acidosis) and decreased at 2% CO_2 (pH 7.8, respiratory alkalosis). At constant CO_2 level (5%), the frequency increased significantly at pH 7.2 (13 mM $NaHCO_3$, metabolic acidosis) and decreased at pH 7.8 (52 mM $NaHCO_3$, metabolic alkalosis). The

Table 1. Effects of respiratory and metabolic acidosis or alkalosis on C4 respiratory rate

	26 mM $NaHCO_3$		
CO_2 (pH)	5% (7.4)	8% (7.2)	2% (7.8)
C4 rate ($n = 54$)	7.5 ± 1.2	11.2 ± 2.1** 5% CO_2	3.3 ± 2.5**
pH ($NaHCO_3$, mM)	7.4 (26)	7.2 (13)	7.8 (52)
C4 rate ($n = 54$)	7.6 ± 1.1	10.6 ± 1.7**	4.8 ± 2.2**

**$P < 0.01$ relative to control. The difference between respiratory alkalosis (26 mM $NaHCO_3$, 2% CO_2) and metabolic alkalosis (5% CO_2, pH 7.8) was not significant.

respiratory frequency tended to be lower with respiratory alkalosis (2% CO_2, 26 mM $NaHCO_3$; pH 7.8) than with metabolic alkalosis (5% CO_2, 52 mM $NaHCO_3$; pH 7.8) but the difference was not significant. Frequency recovered fully over a period of 6–7 min following return to control solution. These results indicate that the respiratory frequency of this preparation was determined mainly by the pH of the superfusate.

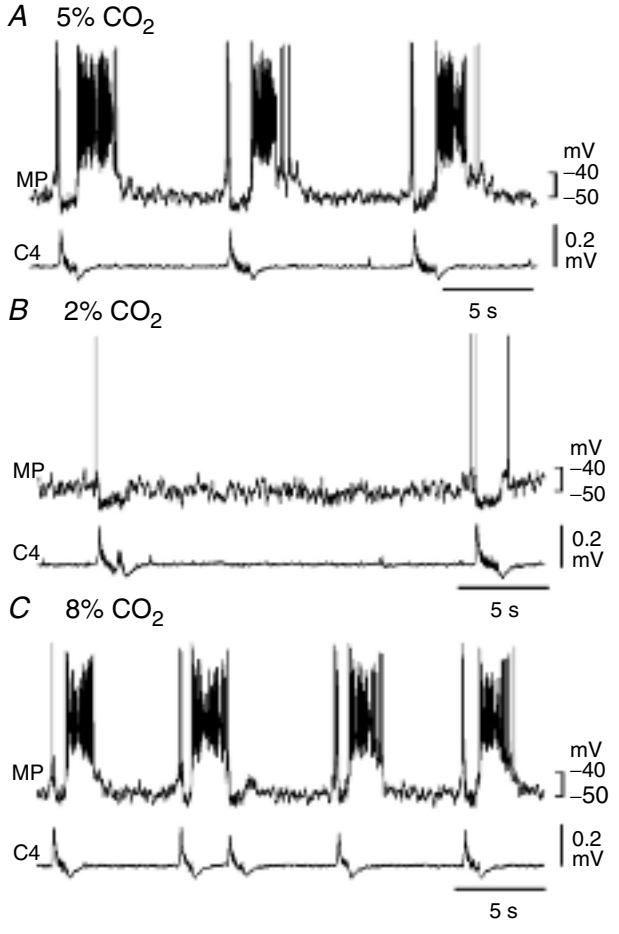

Figure 1. Response of a Pre-I neuron and C4 bursts to respiratory acidosis and alkalosis
Changing the CO_2 concentration of the superfusate from 5% (*A*) to 2% (*B*) or to 8% (*C*) results in alkaline or acidic shifts in pH at the surface of the medulla, a decrease or increase in C4 burst frequency (respiratory frequency) and a corresponding decrease or increase in frequency of rhythmic depolarization of the Pre-I neuron, respectively.

Response of Pre-I neurons to respiratory and metabolic acidosis

Intracellular membrane potentials were recorded from 54 Pre-I neurons. A Pre-I neuron was characterized by a biphasic burst of spikes induced by a depolarizing potential (respiratory drive potential, 2–10 mV) before and after the C4 burst (see Figs 1 and 3). In control CSF, the resting membrane potential was -49 ± 5.2 mV and the input resistance was 610 ± 155 MΩ. These values were similar to our previous data (Onimaru & Homma, 1992).

In Sequence 1, the responses of Pre-I neurons to respiratory acidosis and alkalosis were tested (Table 2). After the control CSF (5% CO_2) was switched to hypocapnic alkaline CSF (2% CO_2), Pre-I neurons hyperpolarized significantly (-2.7 ± 1.6 mV; $P < 0.001$), the amplitude of the drive potential decreased (67%; $P < 0.001$), and the burst rate decreased with a simultaneous decrease in C4 burst frequency. After the CO_2 level was changed from 2% to 8%, Pre-I neurons depolarized ($+6.7 \pm 1.9$ mV; $P < 0.001$) and the amplitude of the drive potential increased (218%; $P < 0.001$) with a simultaneous rise in the burst rate (Fig. 1). These changes in the membrane potential were accompanied by changes in the input resistance and excitatory postsynaptic potentials (EPSPs). Switching to hypocapnic alkaline CSF resulted in a significant decrease of input resistance (83% of control), whereas switching to hypercapnic acidic CSF resulted in a significant increase of input resistance (139% of control) (Table 2). To analyse excitatory postsynaptic currents (EPSCs) of Pre-I neurons, we made voltage-clamp measurements when CO_2 concentration was changed from 2% to 8%. The number of EPSCs increased during all respiratory phases of Pre-I neurons in response to hypercapnia (Fig. 2). We analysed EPSCs during the interburst phase because action potentials during the burst phase could not be clamped sufficiently due to an incomplete space clamp. The frequency of EPSCs during the interburst phase was increased significantly in hypercapnic acidic CSF (5.0 ± 2.6 Hz in 2% CO_2 and 15.0 ± 5.4 Hz in 8% CO_2, $n = 5$; $P < 0.01$). Thus, Pre-I neurons had an excitatory response to respiratory acidosis and an inhibitory response to respiratory alkalosis.

In Sequence 2, the responses of Pre-I neurons to metabolic acidosis and alkalosis were examined. The changes in the resting membrane potential, the burst rate and the EPSPs were similar to those of respiratory acidosis and alkalosis (Table 2). However, the change in the amplitude of the drive potential of Pre-I neurons was

Table 2. Effects of respiratory and metabolic acidosis or alkalosis on membrane properties of Pre-I neurons

	Control	Resp. alkal.	Resp. acid.	Metab. alkal.	Metab. acid.
	5%	2%	8%	pH 7.8	pH 7.2
V_m (mV)	-49.6 ± 4.8	-52.3 ± 3.7 ***	-45.6 ± 3.2***	-51.4 ± 3.8***	-46.5 ± 3.4***
R_m (MΩ)	609 ± 136	506 ± 85**	847 ± 102**	562 ± 93*†††	683 ± 136‡‡‡
Drive potential (mV)	7.3 ± 4.0	4.9 ± 4.5***	10.7 ± 3.7***	6.9 ± 5.0†††	8.2 ± 3.7‡

$n = 17$; *$P < 0.05$; **$P < 0.01$; ***$P < 0.001$ (ANOVA) relative to 5% CO_2, pH 7.4 (Control). †††$P < 0.001$ relative to respiratory alkalosis and ‡$P < 0.05$; ‡‡‡$P < 0.001$ relative to respiratory acidosis (paired *t* test). V_m, membrane potential; R_m, input resistance; Resp. alkal., respiratory alkalosis (2% CO_2, pH 7.8); Resp. acid., respiratory acidosis (8% CO_2, pH 7.2); Metab. alkal., metabolic alkalosis (5% CO_2, pH 7.8); Metab. acid., metabolic acidosis (5% CO_2, pH 7.2).

different from that for respiratory acidosis and alkalosis. Changes of pH from 7.4 to 7.8 or 7.2 at 5% CO_2 induced smaller changes in the drive potential amplitudes (95% for pH 7.4 to 7.8; not significant; 119% for pH 7.8 to 7.2; not significant; Table 2). Moreover, differences of input resistance and drive potential between respiratory and metabolic alkalosis were significant ($P < 0.001$). Similarly, differences of these values between respiratory and metabolic acidosis were significant ($P < 0.05$ for input resistance; $P < 0.001$ for drive potential).

To elucidate the effect of changing CO_2 concentrations at the same pH on the membrane potential of Pre-I neurons on the ventral surface (Sequence 3), hypocapnic alkaline CSF (2% CO_2) was replaced by normocapnic alkaline CSF (5% CO_2) at pH 7.8, and normocapnic acidic CSF (5% CO_2) was replaced by hypercapnic acidic CSF (8% CO_2) at pH 7.2. Figure 3 shows that changes in the CO_2 concentration at the same pH clearly affected the amplitude of the drive potential and intraburst spike frequency. As CO_2 concentration increased, the amplitude of the drive potential and spike frequency increased significantly (Fig. 3 and Table 3). In five of 27 preparations having a low burst rate of less than 1 min^{-1} in 2% CO_2 at pH 7.8, not only the drive potential but also the burst

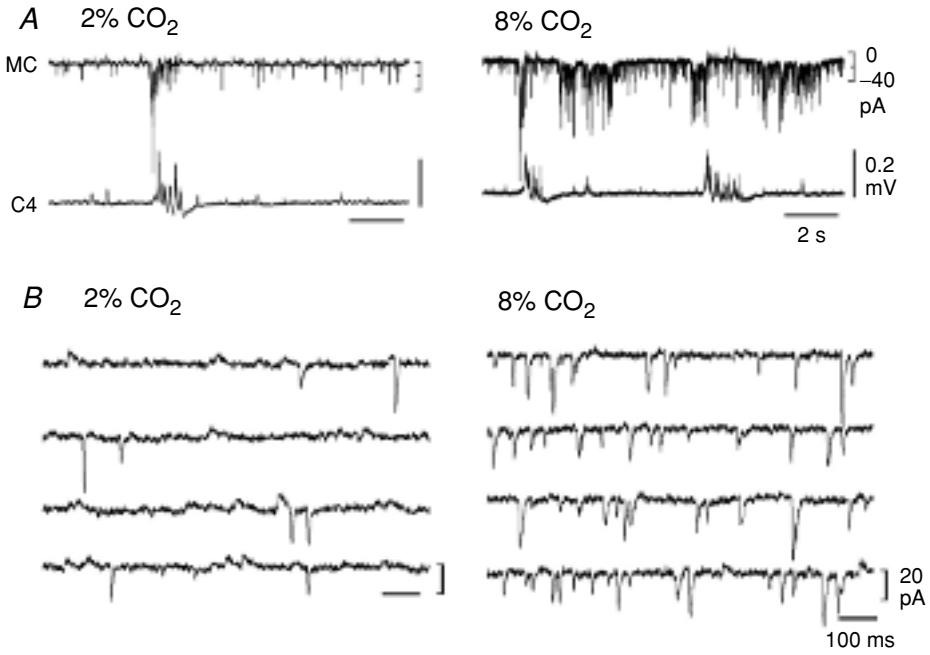

Figure 2. Excitatory synaptic current (EPSC) responses of a Pre-I neuron to respiratory acidosis and alkalosis

A, membrane current (MC) traces of a Pre-I neuron under voltage clamp. Following the change of CO_2 concentration from 2% to 8%, the frequency of EPSCs in the Pre-I neuron increases. *B*, membrane current traces of the same neuron during the interburst phase. The traces show an increase of EPSCs in response to respiratory acidosis.

Table 3. Effects of a change in CO_2 concentration on drive potential and burst phase spike frequency at pH 7.8 or pH 7.2

	pH 7.8		pH 7.2	
CO_2	2% → 5%		5% → 8%	
Drive potential (mV)	5.4 ± 4.5	7.5 ± 4.9***	9.3 ± 3.6	11.2 ± 3.4*
	($n = 15$)		($n = 11$)	
Spike Frequency (Hz)	9.2 ± 6.4	17.3 ± 9.0*	15.3 ± 6.8	20.6 ± 9.4*
	($n = 7$)		($n = 7$)	

*$P < 0.05$; ***$P < 0.001$.

rate and C4 respiratory frequency increased in response to an increase of CO_2 concentration (to 5%) at pH 7.8 (not shown).

Mechanism of the response of Pre-I neurons to respiratory and metabolic acidosis

To determine whether the membrane potential response of Pre-I neurons was mediated intrinsically or synaptically, action potentials were suppressed by the addition of TTX to the superfusate ($n = 41$) in Sequence 4. Figure 4 compares the responses to switching the superfusate from 2% to 8% CO_2 in normal solution (left) and in TTX-containing solution (right). The response in normal solution was a rapid and sustained depolarization of the neuron and an accompanying increase in the burst frequency recorded from the C4 root (Fig. 4*A*). Application of TTX-containing solution had almost no effect on the baseline membrane potential but resulted in a complete suppression of discharge from the C4 root, indicating blockade of synaptic transmission within the respiratory network. Increasing the CO_2 concentration from 2% to 8% resulted in a significant depolarizing response and an increase in the input resistance ($P < 0.001$ by ANOVA) that was not accompanied by discharge in the neuron (Fig. 4*B*, Table 4). Nevertheless, the membrane potential change (ΔV_m) in response to the increase of CO_2 concentration in the presence of TTX was smaller than in the absence of TTX ($P < 0.001$, unpaired student t test; Table 4). These results suggest an involvement of intrinsic

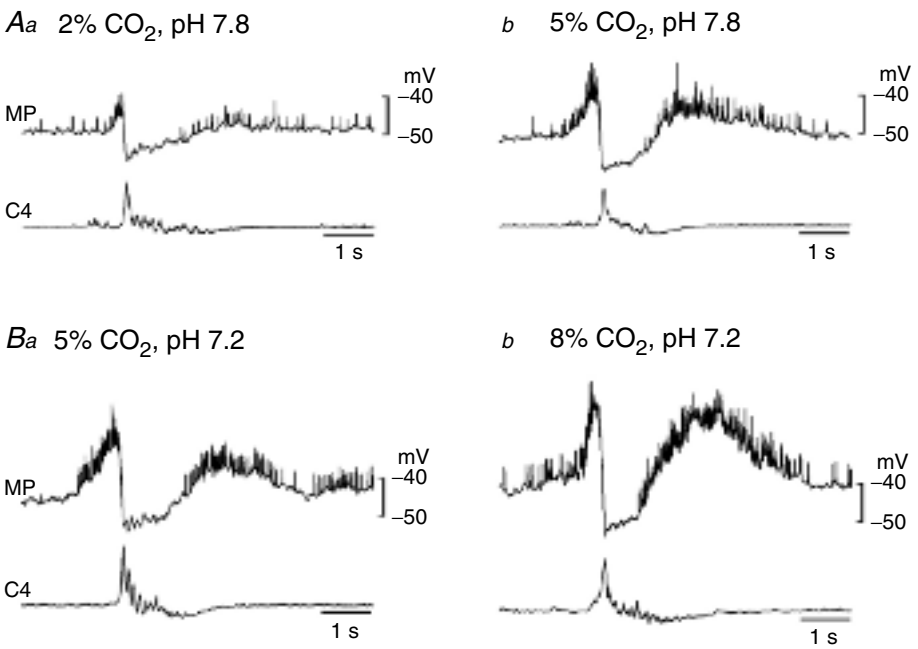

Figure 3. Changes in drive potential of a Pre-I neuron in response to changes in CO_2 concentration at the same pH
Aa and *Ab*, the 2% CO_2 in superfusate (*Aa*) was replaced by 5% CO_2 (*Ab*) at the same pH of 7.8. *Ba* and *Bb*, the 5% CO_2 (*Ba*) was replaced by 8% CO_2 (*Bb*) at the same pH of 7.2. Membrane potential averages from nine respiratory cycles. As CO_2 concentration increases at the same pH, the amplitude of the drive potential and intraburst spike frequency increase. The recordings in *Aa* and *Ab* were made from different neurons to those shown in *Ba* and *Bb*.

Table 4. Effects of respiratory and metabolic acidosis on changes in membrane potential (ΔV_m) and input resistance (ΔR_m) of Pre-I neurons

		Resp. acid.	Metab. Acid.
		($n = 17$)	($n = 17$)
TTX (–)	ΔV_m (mV)	$6.7 \pm 1.9^{***}$	$5.0 \pm 1.8^{***}$
	ΔR_m (MΩ)	$337 \pm 69^{***}$	122 ± 121
		($n = 41$)	($n = 30$)
TTX (+)	ΔV_m (mV)	$2.6 \pm 3.2^{***}$	$2.4 \pm 2.9^{***}$
	ΔR_m (MΩ)	$132 \pm 157^{***}$	42 ± 114
		($n = 8$)	($n = 7$)
TTX + Cd^{2+}	ΔV_m (mV)	$6.6 \pm 2.4^{**}$	$5.2 \pm 1.5^{**}$
	ΔR_m (MΩ)	$323 \pm 53^{***}$	131 ± 175
		($n = 8$)	($n = 7$)
TTX + Cd^{2+} + Ba^{2+}	ΔV_m (mV)	-0.03 ± 0.4	$2.9 \pm 2.4^{**}$
	ΔR_m (MΩ)	20 ± 41	19 ± 49
		($n = 8$)	($n = 7$)

$^{**}P < 0.01$; $^{***}P < 0.001$ relative to Control (respiratory alkalosis or metabolic alkalosis) (ANOVA). Resp. acid., respiratory acidosis (from 2% CO_2, pH 7.8 to 8% CO_2, pH 7.2); Metab. alkal.; Metab. acid., metabolic acidosis (from 5% CO_2, pH 7.8 to 5% CO_2, pH 7.2)

channel mechanism in response to increased CO_2 level as well as a considerable contribution of synaptic mechanism. These results also suggest that Pre-I neurons may consist of heterogeneous subpopulations with regard to CO_2 responsiveness. Indeed, the depolarizing response of some Pre-I neurons (15 of 41) to respiratory acidosis (6.3 ± 2.5 mV) was fully retained after the suppression of synaptic transmission (6.7 ± 3.1 mV), suggesting that the response might be mediated mainly by an intrinsic mechanism in those 15 Pre-I neurons.

Metabolic acidosis (change of pH from 7.8 to 7.2 at 5% CO_2, $n = 30$) also induced a significant depolarization in

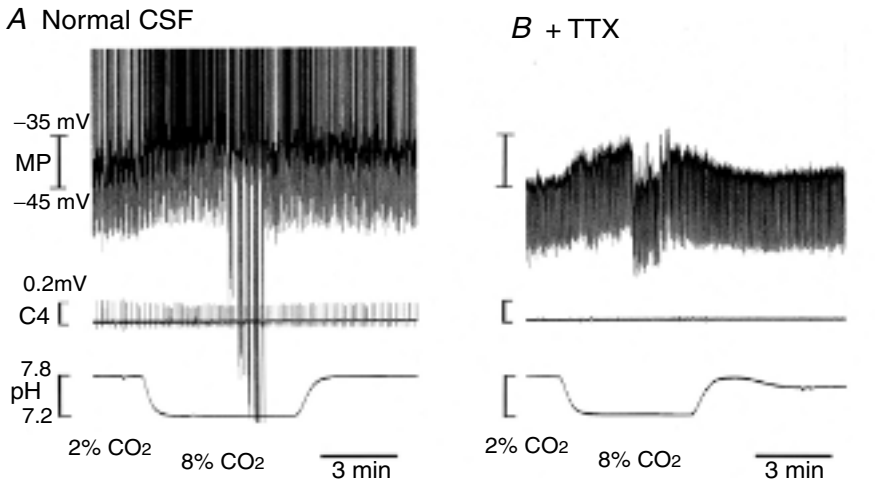

Figure 4. Depolarizing response of a Pre-I neuron to respiratory acidosis is retained after respiratory rhythm is suppressed by TTX

A, switching the superfusate from 2% to 8% CO_2 results in a rapid and sustained depolarization of a Pre-I neuron and an accompanying increase in the burst frequency recorded on the C4 root. *B*, the addition of 1 μM TTX has almost no effect on the baseline membrane potential but results in a complete suppression of discharge on the C4 root. Increasing the CO_2 concentration results in a depolarizing response that was not accompanied by discharge. The membrane potential was measured during periodic current injection (1 Hz, 50 pA) to test the response of input resistance to the change in CO_2 level. The negative deflections of the baseline membrane potential in each panel are proportional to the input resistance; the large negative deflections in the centre of panel *A* occurred during measurement of the *I–V* curve of the neuron. To compare input resistances at the same membrane potential, the membrane potential of the neuron in 8% CO_2 was adjusted to the same level as in 2% CO_2 by negative current injection (panel *B*). Note the increase in input resistance of the neuron in 8% CO_2.

the presence of TTX, whereas change in the input resistance (ΔR_m) was not significant (Fig. 5; Table 4). The ΔV_m in response to metabolic acidosis in TTX was smaller than that in the absence of TTX ($P < 0.01$, unpaired student *t* test; Table 4). Moreover, ΔR_m in metabolic acidosis was smaller than that in respiratory acidosis ($P < 0.01$, unpaired student *t* test; Table 4). Indeed, five of the 12 neurons showing depolarization similar to that in response to metabolic acidosis before application of TTX did not show any increase in the input resistance (Fig. 5). These results suggest that there are different channel mechanisms for the membrane potential responses to respiratory and metabolic acidosis.

To investigate the channel mechanisms mediating the acidosis responses, an inorganic calcium channel blocker (Cd^{2+}) and potassium channel blocker (Ba^{2+}) were added to the superfusate after addition of TTX, and the responses of Pre-I neurons to both respiratory and metabolic acidosis were tested (Sequence 4). Only the neurons that had a depolarizing shift in membrane potential after addition of TTX ($n = 15$) were tested in this protocol. Figure 6 illustrates the effect of TTX, Cd^{2+} and Ba^{2+} on the membrane potential response for respiratory (upper) and metabolic (lower) acidosis. In all Pre-I neurons during respiratory acidosis ($n = 8$), Ba^{2+} alone blocked the depolarizing shift in membrane potential and the increase in input resistance (Fig. 6, upper panel and Table 4). Thus, the potassium channel seems to be responsible for the depolarizing response of Pre-I neurons to respiratory acidosis. However, in response to metabolic acidosis ($n = 7$), neurons were depolarized significantly without change in input resistance even after addition of Cd^{2+} and Ba^{2+} (Fig. 6, lower panel and Table 4). Thus, the channel mechanisms that account for the depolarizing response might be different for respiratory and metabolic acidosis.

To study the response of intrinsic burst activity of Pre-I neurons to respiratory or metabolic acidosis, membrane potential was recorded in low-Ca solution and the response to respiratory or metabolic acidosis was tested with Sequence 5 ($n = 4$). The change from control to low-Ca solution caused a slight depolarizing shift of the baseline membrane potential and increased the phasic burst frequency with a complete suppression of discharge from the C4 root. Both respiratory and metabolic acidosis resulted in a depolarizing shift in membrane potential and an increase in phasic burst frequency that was accompanied by discharge in the neuron (Figs 7 and 8). A similar response was observed when the neuron was depolarized with positive current injection (Fig. 8*C*). This shows that the depolarizing shift of the resting membrane potential of the Pre-I neurons increased the burst frequency of the phasic depolarization.

Histological findings

All cell bodies of Pre-I neurons ($n = 22$; Fig. 9) were located in the rostral ventrolateral medulla. The region examined in the present study corresponded to the caudal part of the pFRG and was within 200 μm caudal to the caudal end of the facial nucleus. The depth of the cell bodies from the ventral surface was 90–400 μm. The longer axis of the cell body was 17–28 μm. Pre-I neurons had three to five primary dendrites, some of which projected towards the

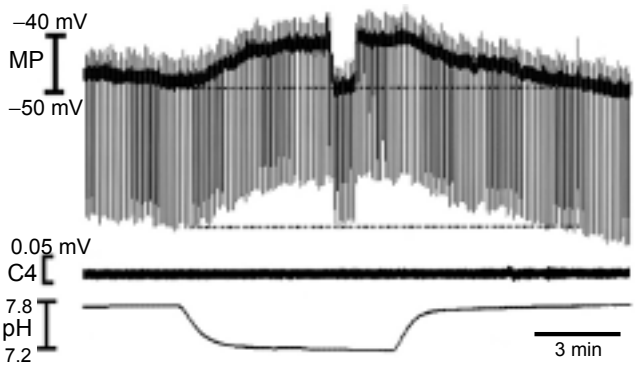

Figure 5. Membrane potential response of a Pre-I neuron to metabolic acidosis after suppression of synaptic transmission by TTX
Following addition of 1 μM TTX, the depolarizing shift in membrane potential of a Pre-I neuron in response to metabolic acidosis persists. However, the input resistance response is different from that for respiratory acidosis (see Fig. 4*B*). The input resistance of the neuron does not increase during metabolic acidosis. Note that the magnitudes of negative deflections at both pH levels are the same (dotted lines).

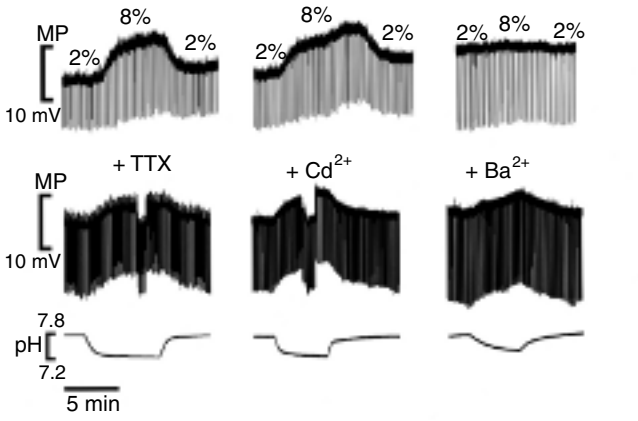

Figure 6. Channel mechanisms that account for the depolarizing responses induced by respiratory and metabolic acidosis
Upper panels show responses of a Pre-I neuron to respiratory acidosis after addition of 1 μM TTX, 0.1 mM Cd^{2+} and 1 mM Ba^{2+}; lower panels illustrate responses to metabolic acidosis. In respiratory acidosis (upper panel), only Ba^{2+} affects the depolarizing shift in membrane potential of the Pre-I neuron. However, in metabolic acidosis (lower panel), neither Cd^{2+} nor Ba^{2+} affects the depolarizing membrane potential response.

ventral surface. There were no morphological differences between neurons that had intrinsic and synaptic responses to CO_2/H^+.

Discussion

We found that the Pre-I neuron, the putative respiratory rhythm generator, is intrinsically and synaptically chemosensitive to both CO_2 and H^+. We also found that the intrinsic responses are mediated by potassium channels during respiratory acidosis and by another mechanism during metabolic acidosis. Pre-I neurons are potentially able to modulate the respiratory rhythm in response to CO_2/H^+ changes in the brainstem–spinal cord preparation.

Although it has been shown that the medullary respiratory network remains functionally intact in the isolated brainstem–spinal cord preparation of the neonatal rat (Suzue, 1984; Smith *et al.* 1990), the relation between the rhythm generated by the *in vitro* brainstem and that generated *in vivo* is not understood in detail. Moreover, we did not study the response of pacemaker neurons in the pre-Bötzinger complex (advocated by Smith *et al.* 1991) to changes in CO_2/H^+. Thus, we emphasize that considerable care should be exercised in extrapolating our experimental data to *in vivo* conditions.

Differences in responses of Pre-I neurons to respiratory acidosis and metabolic acidosis

The burst frequency of Pre-I neurons and the respiratory frequency of this preparation depend mainly on the pH of the superfusate. This conclusion is consistent with previous studies with this preparation (Onimaru *et al.* 1989; Kawai *et al.* 1996). Nevertheless, a change in CO_2 concentration at the same pH level could affect these parameters in a situation where respiration was reduced at alkaline pH. Voipio & Ballanyi (1997) reported a similar effect on respiratory frequency and proposed a direct effect of CO_2. When the stimulation of the respiratory network by H^+ ion is reduced, the effect of CO_2 on respiratory frequency may be apparent.

The effects on the amplitude of the drive potential of Pre-I neurons differed between respiratory acidosis and metabolic acidosis. A change in CO_2 concentration resulted in a marked change in the amplitude of the drive potential of Pre-I neurons, whereas a pH change at the same 5% CO_2 level induced a relatively smaller change

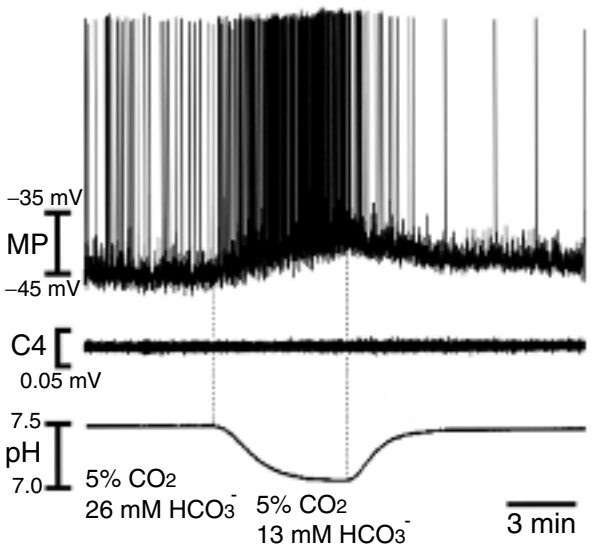

Figure 7. Response of a Pre-I neuron to metabolic acidosis after suppression of synaptic transmission in low-Ca^{2+}, high-Mg^{2+} superfusate
Metabolic acidosis results in a depolarizing shift in membrane potential and an increase in firing frequency, although the C4 burst is fully suppressed by low-Ca^{2+}, high-Mg^{2+} solution.

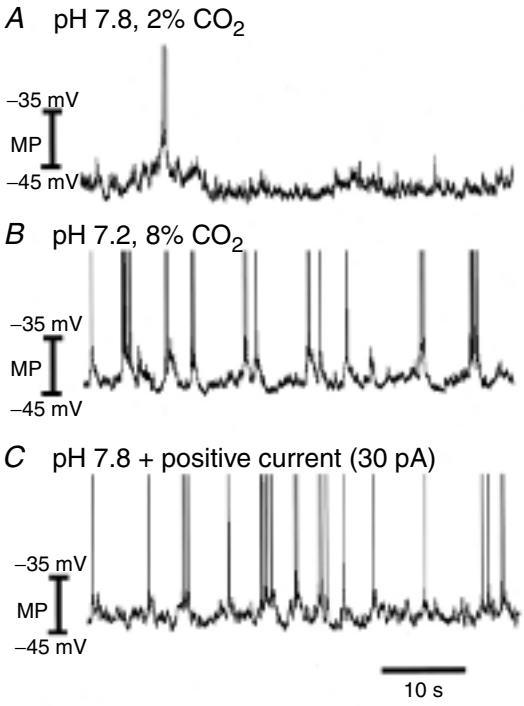

Figure 8. Response of burst frequency of a Pre-I neuron to respiratory acidosis in low-Ca^{2+}, high-Mg^{2+} superfusate
Respiratory acidosis results in a depolarizing shift in membrane potential and an increase in phasic burst frequency that is accompanied by discharge in the neuron (*A* and *B*). A similar response is observed when the neuron is depolarized with positive current injection (*C*). Note that the burst frequency of the Pre-I neuron increases with membrane depolarization.

in drive potential. Moreover, even at the same pH at the medullary surface, a change in CO_2 level clearly affected the amplitude of the drive potential. As CO_2 concentration increased at the same pH at the surface, the amplitude of the drive potential increased. We measured only the surface pH and did not measure the tissue pH where the neurons were located. Our preliminary experiments and a previous study (Okada *et al.* 1993*a*) showed that a change in pH induced by a change in CO_2 concentration was much faster than that induced by a change in bicarbonate concentration even at a depth of 100–200 μm from the surface where most Pre-I neurons are located. However, 5 min after a change of bath CO_2 concentration and 10 min after a change of bicarbonate concentration, the tissue pH stabilized. In the present experiments, we examined the effects of a change in CO_2 concentration 10 min after the change of the bath solution. Moreover, the tissue pH change induced by a change in CO_2 concentration was slightly smaller than that induced by a change in bicarbonate concentration (Okada *et al.* 1993*a*). Therefore, respiratory acidosis might induce smaller acidic shifts in the regions where the cell bodies are located than those induced by metabolic acidosis. Thus, it is possible that the CO_2 molecule itself affects the drive potential of Pre-I neurons, although further study will be necessary to obtain a definite result and elucidate the mechanisms involved.

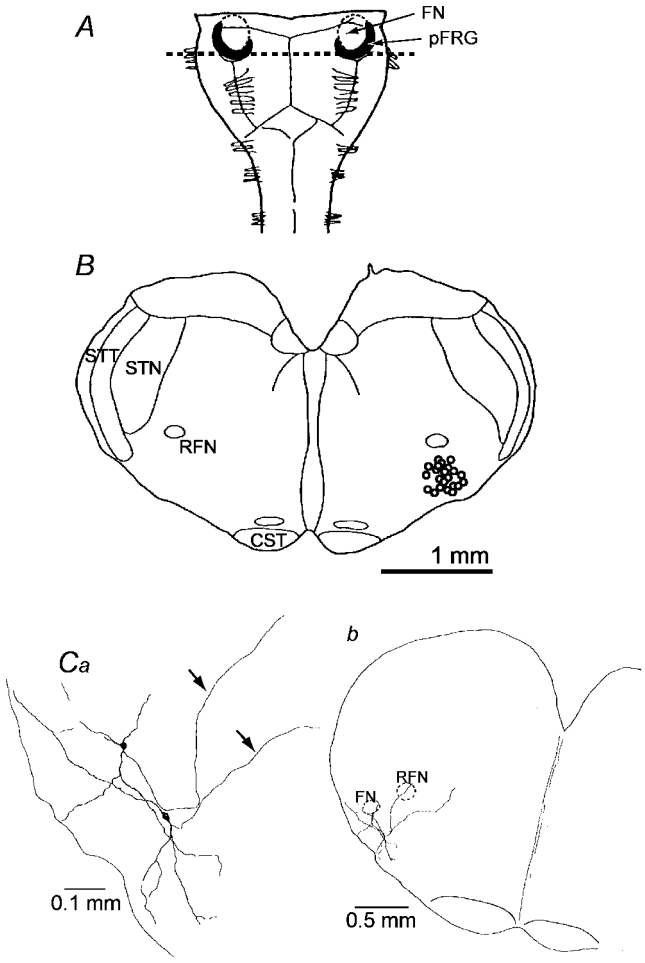

Figure 9. Location of recorded neurons
A, ventral aspect of preparation and approximate area of para-facial respiratory group (pFRG). *B*, location of recorded neurons stained with Lucifer Yellow, plotted in a section denoted by dotted lines in *A*. *C*, examples of Lucifer Yellow-filled cells. Some dendrites reached the ventral surface. Arrows show axons. CST, corticospinal tract; FN, facial nucleus; RFN, retrofacial nucleus; STN, spinal trigeminal nucleus; STT, spinal trigeminal tract.

These differences in response to respiratory and metabolic acidosis have not previously been observed in respiratory modulated neurons. Takeda & Haji (1991) reported that respiratory acidosis increased the amplitude of phasic depolarization in inspiratory and post-inspiratory neurons in the ventral respiratory group of an *in vivo* cat preparation, although they did not examine the effect of metabolic acidosis. Wang *et al.* (2002) performed systematic experiments to determine the primary stimulus for chemosensitive neurons located in the medullary raphe nuclei. They suggested that a change in intracellular pH might be the primary stimulus for chemosensitivity in the neurons because chemosensitivity of raphe neurones can occur independently of changes in CO_2 level, extracellular pH or bicarbonate level. This may be the case for the response to respiratory acidosis in Pre-I neurons because CO_2 induces an intracellular acidification much faster than H^+.

Synaptic mechanisms of CO_2/H^+ chemoreception of Pre-I neurons

The drive potential is a mixture of membrane potential fluctuations caused by synaptic potentials and activation of intrinsic conductance (Onimaru *et al.* 2003). The contribution of intrinsic conductance to pH effects was examined in the presence of TTX (see below). The contribution of synaptic potentials was analysed under voltage clamp. Although the space clamp was incomplete, especially during the burst phase, the results indicated that the frequency of EPSCs increased in response to an increase in CO_2 concentration. The origin of neurons sending these EPSCs is unknown, but other Pre-I neurons and tonically active chemosensitive neurons in the RTN (Mulkey *et al.* 2004; Li & Nattie, 2002) and other brainstem regions (Richerson, 2004) should be considered (see below).

Intrinsic mechanisms of CO_2/H^+ chemoreception of Pre-I neurons

Because the depolarizing response and increase in the input resistance of Pre-I neurons to respiratory acidosis was retained after the suppression of synaptic

transmission, our findings suggested that the response was mediated by an intrinsic mechanism. However, the results do not exclude the possible involvement of action potential-independent release of neuromodulators (e.g. Gourine *et al.* 2005) in the depolarizing response to respiratory acidosis. The response of the input resistance to a change in CO_2 concentration was also retained in these neurons, further suggesting the contribution of an intrinsic channel mechanism in the membrane potential response. The response of the other neurons was a markedly decreased depolarizing shift in membrane potential after suppression of synaptic transmission, suggesting involvement of a synaptic mechanism.

Further study of the channel mechanisms found that a potassium channel blocker (Ba^{2+}), in the presence of TTX, completely blocked the depolarizing shift in membrane potential of Pre-I neurons during respiratory acidosis and did not block it during metabolic acidosis, whereas an inorganic calcium channel blocker (Cd^{2+}) had no significant effect. Thus, a decrease in the potassium conductance seems to be responsible for the depolarizing response of Pre-I neurons to respiratory acidosis.

Recently, a CO_2/H^+ chemosensitive potassium channel consisting of two members of the inward rectifier potassium channel family (Kir4.1 and Kir5.1) was reported by Xu *et al.* (2000). This potassium channel family enables neurons to detect intracellular acidification induced by hypercapnia and is expressed in brainstem neurons. If Pre-I neurons have Kir4.1 and Kir5.1 in their membranes, the intrinsic response to hypercapnia might be mediated by the CO_2-sensitive inward rectifier potassium channel.

Because H^+ is much less membrane-permeable than CO_2, metabolic acidosis may not easily induce intracellular acidification of Pre-I neurons. This could explain why the responses of Pre-I neurons to respiratory acidosis and metabolic acidosis are different. Moreover, another family of putative leak potassium channels (KCNK) has been identified by molecular cloning (reviewed by Goldstein *et al.* 2001; Patel & Honore, 2001). Among these, subgroups of so-called TASK channel currents are inhibited by extracellular protons in a physiological pH range. TASK channel currents were found in neurons of the locus coeruleus and medullary raphe (Talley *et al.* 2000; Bayliss *et al.* 2001). If Pre-I neurons possess TASK channels, extracellular acidification would be able to modulate their resting membrane potentials. Some cases of metabolic acidosis might induce the depolarization of Pre-I neurons by this mechanism.

However, in response to metabolic acidosis, Pre-I neurons retained their depolarizing response following the blockade of both calcium and potassium channels. Such a response might be mediated by other intrinsic mechanisms not involving membrane conductance changes; however, these could not be identified in the present study. We suggest that the intrinsic mechanisms that account for the depolarizing responses of Pre-I neurons are different for respiratory and metabolic acidosis.

The mechanisms modulating respiratory activity in response to CO_2/H^+: functional considerations

CO_2/H^+ changes in a superfusate clearly affect the respiratory frequency of this preparation (Okada *et al.* 1993*b*; Kawai *et al.* 1996). We and other groups have provided evidence that the RVL plays a pivotal role in rhythmogenesis of respiration in the brainstem–spinal cord preparation (Onimaru *et al.* 1987; Errchidi *et al.* 1991). The neuronal network in the RVL that includes Pre-I neurons, recently renamed pFRG (Onimaru & Homma, 2003), is involved primarily in generation of the respiratory rhythm (Ballanyi *et al.* 1999). After suppression of synaptic transmission, some Pre-I neurons in the RVL showed rhythmic changes in membrane potentials (phasic bursts; see also Onimaru *et al.* 1995); the frequencies of the phasic bursts depended on their baseline membrane potentials, which were affected by CO_2/H^+ changes (Fig. 8; Onimaru *et al.* 1989). Such Pre-I neurons in the RVL possess an intrinsic burst-generating property. It has been reported that the respiratory frequency of this preparation closely correlated with the burst frequency of Pre-I neurons (Onimaru *et al.* 1998; Takeda *et al.* 2001; Mellen *et al.* 2003). Thus, the depolarizing response to increased CO_2 concentration or decreased pH might directly result in an increase in respiratory frequency in the brainstem–spinal cord preparation. However, because we did not examine pacemaker neurons in the pre-Bötzinger complex (Smith *et al.* 1991), there remains a possibility that they also modulate respiratory frequency in response to CO_2/H^+ changes.

Of the many neurons, besides Pre-I neurons, that respond intrinsically to CO_2/H^+, at least three groups may be the primary chemosensors of respiration. The first group consists of relatively small neurons discovered by Okada *et al.* (2002). These neurons, which might be cholinergic (Chen *et al.* 1997), are located just beneath the surface of the ventral medulla and are connected to the deeper region. The second group consists of glutamatergic neurons, which are located in the retrotrapezoid nucleus in the rostral ventrolateral medulla; their pH sensitivity is intrinsic and involves a background K^+ current (Mulkey *et al.* 2004). The third group consists of the serotonergic neurons in the ventral medulla that stimulate the neuronal network that controls breathing (Richerson, 2004). Pre-I neurons and the respiratory activity of this preparation are affected by serotonin (Onimaru *et al.* 1998). Recently, Gourine *et al.* (2005) suggested that release of ATP from the classical brainstem chemosensitive area participates to mediate the effect of CO_2 on breathing. They stated that the immediate release of ATP from the chemosensitive

structure plays a key role in central chemoreception. However, they did not elucidate the cellular sources and mechanisms underlying release of ATP in response to an increase in CO_2 level. ATP also stimulates both Pre-I neurons and the respiratory activity of this preparation (A. Kawai, unpublished data). As Li & Nattie (2002) reported, multiple chemoreceptor sites and structures may interact to provide high CO_2 chemosensitivity. Excitatory synaptic inputs onto Pre-I neurons were increased in response to increased CO_2 concentration and decreased pH, and some Pre-I neurons were synaptically chemosensitive. Such Pre-I neurons might be stimulated by the superficial cholinergic, glutamatergic or serotonergic neurons and by the ATP-releasing structure in the medullary surface.

In conclusion, the frequency of the rhythmic respiratory bursts of Pre-I neurons is dependent on the baseline membrane potential that is modulated by the level of CO_2/H^+ as a result of the integration of both intrinsic membrane mechanisms and synaptic mechanisms. Thus, Pre-I neurons could contribute to control of respiratory frequency during central CO_2/H^+ chemoreception.

References

Arata A, Onimaru H & Homma I (1990). Respiration-related neurons in the ventral medulla of newborn rats in vitro. *Brain Res Bull* **24**, 599–604.

Ballanyi K, Onimaru H & Homma I (1999). Respiratory network function in the isolated brainstem-spinal cord of newborn rats. *Prog Neurobiol* **59**, 583–634.

Bayliss DA, Talley EM, Sirois JE & Lei Q (2001). TASK-1 is a highly modulated pH-sensitive 'leak' K^+ channel expressed in brainstem respiratory neurons. *Respir Physiol* **129**, 159–174.

Chen Z, Okada Y & Eldridge FL (1997). Hypercapnia-induced c-fos expression in cholinergic cells within the marginal glial layer of the rat ventral medulla oblongata. *FASEB J* **11**, A131.

Coates EL, Li A & Nattie EE (1993). Widespread sites of brain stem ventilatory chemoreceptors. *J Appl Physiol* **75**, 5–14.

Dean JB, Bayliss DA, Erickson JT, Lawing WL & Millhorn DE (1990). Depolarisation and stimulation of neurons in the nucleus tractus solitarii by carbon dioxide does not require chemical synaptic input. *Neuroscience* **36**, 207–216.

Dean JB, Lawing WL & Millhorn DE (1989). CO_2 decreases membrane conductance and depolarizes neurons in the nucleus tractus solitarii. *Exp Brain Res* **76**, 656–661.

Errchidi S, Monteau R & Hilaire G (1991). Noradrenergic modulation of the medullary respiratory rhythm generator in the newborn rat: an in vitro study. *J Physiol* **443**, 477–498.

Feldman JL, Mitchell GS & Nattie EE (2003). Breathing: rhythmicity, plasticity, chemosensitivity. *Annu Rev Neurosci* **26**, 239–266.

Goldstein SA, Bockenhauer D, O'Kelly I & Zilberberg N (2001). Potassium leak channels and the KCNK family of two-P-domain subunits. *Nat Rev Neurosci* **2**, 175–184.

Gourine AV, Llaudet E, Dale N & Spyer KM (2005). ATP is a mediator of chemosensory transduction in the central nervous system. *Nature* **436**, 108–111.

Harada Y, Kuno M & Wang YZ (1985). Differential effects of carbon dioxide and pH on central chemoreceptors in the rat in vitro. *J Physiol* **368**, 679–693.

Issa FG & Remmers JE (1992). Identification of a subsurface area in the ventral medulla sensitive to local changes in PCO_2. *J Appl Physiol* **72**, 439–446.

Kawai A, Ballantyne D, Mückenhoff K & Scheid P (1996). Chemosensitive medullary neurones in the brainstem-spinal cord preparation of the neonatal rat. *J Physiol* **492**, 277–292.

Kawai A, Onimaru H, Arata A & Homma I (1997). A role of preinspiratory neuron of the central chemo-sensitivity of respiration in the brainstem-spinal cord preparation. *Jpn J Physiol* **47**, S96.

Li A & Nattie E (2002). CO_2 dialysis in one chemoreceptor site, the RTN: stimulus intensity and sensitivity in the awake rat. *Respir Physiol Neurobiol* **133**, 11–22.

Li A, Randall M & Nattie EE (1999). CO_2 microdialysis in the retrotrapezoid nucleus of the rat increases breathing in wakefulness but not in sleep. *J Appl Physiol* **87**, 910–919.

Loeschcke HH (1982). Central chemosensitivity and the reaction theory. *J Physiol* **332**, 1–24.

Loeschcke HH, De Lattre J, Schlaefke ME & Trouth CO (1970). Effects on respiration and circulation of electrically stimulating the ventral surface of the medulla oblongata. *Respir Physiol* **10**, 184–197.

Mellen NM, Janczewski WA, Bocchiaro CM & Feldman JL (2003). Opioid-induced quantal slowing reveals dual networks for respiratory rhythm generation. *Neuron* **37**, 821–826.

Mitchell RA, Loeschcke HH, Massion WH & Severinghaus JW (1963). Respiratory responses mediated through superficial chemosensitive areas on the medulla. *J Appl Physiol* **18**, 523–533.

Mulkey DK, Stornetta RL, Weston MC, Simmons JR, Parker A, Bayliss DA & Guyenet PG (2004). Respiratory control by ventral surface chemoreceptor neurons in rats. *Nat Neurosci* **7**, 1360–1369.

Nattie E (1999). CO_2, brainstem chemoreceptors and breathing. *Prog Neurobiol* **59**, 299–331.

Nattie E (2000). Multiple sites for central chemoreception: their roles in response sensitivity and in sleep and wakefulness. *Respir Physiol* **122**, 223–235.

Nattie EE (2001). Central chemosensitivity, sleep, and wakefulness. *Respir Physiol* **129**, 257–268.

Nattie EE & Li A (2002). CO_2 dialysis in nucleus tractus solitarius region of rat increases ventilation in sleep and wakefulness. *J Appl Physiol* **92**, 2119–2130.

Okada Y, Chen Z, Jiang W, Kuwana S & Eldridge FL (2002). Anatomical arrangement of hypercapnia-activated cells in the superficial ventral medulla of rats. *J Appl Physiol* **93**, 427–439.

Okada Y, Mückenhoff K, Holtermann G, Acker H & Scheid P (1993*a*). Depth profiles of pH and PO_2 in the isolated brainstem-spinal cord of the neonatal rat. *Respir Physiol* **93**, 315–326.

Okada Y, Mückenhoff K & Scheid P (1993*b*). Hypercapnia and medullary neurons in the isolated brainstem-spinal cord of the rat. *Respir Physiol* **93**, 327–336.

Onimaru H, Arata A & Homma I (1987). Localization of respiratory rhythm-generating neurons in the medulla of brainstem-spinal cord preparations from newborn rats. *Neurosci Lett* **78**, 151–155.

Onimaru H, Arata A & Homma I (1989). Firing properties of respiratory rhythm generating neurons in the absence of synaptic transmission in rat medulla in vitro. *Exp Brain Res* **76**, 530–536.

Onimaru H, Arata A & Homma I (1995). Intrinsic burst generation of preinspiratory neurons in the medulla of brainstem-spinal cord preparations isolated from newborn rats. *Exp Brain Res* **106**, 57–68.

Onimaru H, Ballanyi K & Homma I (2003). Contribution of Ca^{2+}-dependent conductances to membrane potential fluctuations of medullary respiratory neurons of newborn rats *in vitro*. *J Physiol* **552**, 727–741.

Onimaru H & Homma I (1992). Whole cell recordings from respiratory neurons in the medulla of brainstem-spinal cord preparations isolated from newborn rats. *Pflugers Arch* **420**, 399–406.

Onimaru H & Homma I (2003). A novel functional neuron group for respiratory rhythm generation in the ventral medulla. *J Neurosci* **23**, 1478–1486.

Onimaru H, Shamoto A & Homma I (1998). Modulation of respiratory rhythm by 5-HT in the brainstem-spinal cord preparation from newborn rat. *Pflugers Arch* **435**, 485–494.

Oyamada Y, Ballantyne D, Mückenhoff K & Scheid P (1998). Respiration-modulated membrane potential and chemosensivity of locus coeruleus neurons in the in vitro brainstem-spinal cord of the neonatal rat. *J Physiol* **513**, 381–398.

Patel AJ & Honore E (2001). Properties and modulation of mammalian 2P domain K^+ channels. *Trends Neurosci* **24**, 339–346.

Richerson GB (2004). Serotonergic neurons as carbon dioxide sensors that maintain pH homeostasis. *Nat Rev Neurosci* **5**, 449–461.

Schlaefke ME, See WR & Loeschcke HH (1970). Ventilatory response to alterations of H^+ ion concentration in small areas of the ventral medullary surface. *Respir Physiol* **10**, 198–212.

Smith JC, Ellenberger HH, Ballanyi K, Richter DW & Feldman JL (1991). Pre-Bötzinger complex: a brainstem region that may generate respiratory rhythm in mammals. *Science* **254**, 726–729.

Smith JC, Greer JJ, Liu GS & Feldman JL (1990). Neural mechanisms generating respiratory pattern in mammalian brainstem-spinal cord in vitro. I. Spatiotemporal patterns of motor and medullary neuron activity. *J Neurophysiol* **64**, 1149–1169.

Suzue T (1984). Respiratory rhythm generation in the in vitro brain stem-spinal cord preparation of the neonatal rat. *J Physiol* **354**, 173–183.

Takeda R & Haji A (1991). Synaptic response of bulbar respiratory neurons to hypercapnic stimulation in peripherally chemodenervated cats. *Brain Res* **561**, 307–317.

Takeda S, Eriksson LI, Yamamoto Y, Joensen H, Onimaru H & Lindahl SG (2001). Opioid action on respiratory neuron activity of the isolated respiratory network in newborn rats. *Anesthesiology* **95**, 740–749.

Talley EM, Lei Q, Sirois JE & Bayliss DA (2000). TASK-1, a two-pore-domain K^+ channel, is modulated by multiple neurotransmitters in motoneurons. *Neuron* **25**, 399–410.

Voipio J & Ballanyi K (1997). Interstitial PCO_2 and pH, and their role as chemostimulants in the isolated respiratory network of neonatal rats. *J Physiol* **499**, 527–542.

Wang W, Bradley SR & Richerson GB (2002). Quantification of the response of rat medullary raphe neurones to independent changes in pH_o and PCO_2. *J Physiol* **540**, 951–970.

Xu H, Cui N, Yang Z, Qu Z & Jiang C (2000). Modulation of kir4.1 and kir5.1 by hypercapnia and intracellular acidosis. *J Physiol* **524**, 725–735.

Acknowledgements

The study was supported by Grants-in-Aid for Scientific Research from the Ministry of Education, Science and Culture in Japan.